Cell, Vol. 105, 391–402, May 4, 2001, Copyright ©2001 by Cell Press

The Structure of the β-Catenin/E-Cadherin Complex and the Molecular Basis of Diverse Ligand Recognition by β-Catenin

Andrew H. Huber and William I. Weis[1]
Departments of Structural Biology and Molecular and Cellular Physiology
Stanford University School of Medicine
299 Campus Drive West
Stanford, California 94305

Summary

As a component of adherens junctions and the Wnt signaling pathway, β-catenin binds cadherins, Tcf family transcription factors, and the tumor suppressor APC. We have determined the crystal structures of both unphosphorylated and phosphorylated E-cadherin cytoplasmic domain complexed with the arm repeat region of β-catenin. The interaction spans all 12 arm repeats, and features quasi-independent binding regions that include helices which interact with both ends of the arm repeat domain and an extended stretch of 14 residues which closely resembles a portion of XTcf-3. Phosphorylation of E-cadherin results in interactions with a hydrophobic patch of β-catenin that mimics the binding of an amphipathic XTcf-3 helix. APC contains sequences homologous to the phosphorylated region of cadherin, and is likely to bind similarly.

Introduction

The cytosolic protein β-catenin has essential roles in cell adhesion and in signal transduction. β-catenin is a component of adherens junctions, sites of cell-cell contact in which the actin cytoskeletons of adjacent cells are linked through cadherin cell adhesion molecules (Yap et al., 1997a). β-catenin binds to the cytoplasmic domain of classical cadherins and to α-catenin, which in turn binds directly to F-actin and other actin-associated proteins. A similar assembly exists in desmosomes, where the cytoplasmic domain of desmosomal cadherins binds to the β-catenin homolog plakoglobin. Cell junctions are dynamic and regulated assemblies, and several mechanisms, including phosphorylation of junction components, appear to control cadherin-based adhesion (Gumbiner, 2000). Phosphorylation of E-cadherin enhances cell adhesiveness and the affinity of the E-cadherin/β-catenin complex (Lickert et al., 2000).

β-catenin is also a transcriptional coactivator in the Wnt growth factor signaling pathway that controls cell fate determination (Polakis, 2000). In the absence of Wnt, phosphorylation by glycogen synthase kinase-3β (GSK-3β) targets β-catenin for degradation (Aberle et al., 1997; Orford et al., 1997). Phosphorylation of β-catenin by GSK-3β occurs in a multiprotein complex that includes the tumor suppressor Adenomatous Polyposis Coli (APC) and Axin, both of which bind to β-catenin. Wnt inhibits GSK-3β-mediated phosphorylation of β-catenin. Under these conditions, β-catenin enters the nucleus and forms complexes with transcription factors of the LEF/Tcf family, resulting in transcriptional activation.

The primary structure of β-catenin consists of an amino terminal domain of 149 amino acids, followed by a central domain of 515 residues composed of 12 armadillo (arm) repeats, and a C-terminal 108 residue domain. The arm repeat domain mediates the binding of β-catenin to cadherins (Hülsken et al., 1994; Pai et al., 1996), APC (Hülsken et al., 1994; Rubinfeld et al., 1995), Axin (Behrens et al., 1998; Ikeda et al., 1998), and Tcf family transcription factors (Behrens et al., 1996; van de Wetering et al., 1997). The crystal structure of the arm repeat domain showed that each arm repeat consists of three helices, designated H1, H2, and H3 (Huber et al., 1997). The repeats pack against one another to form a superhelix that features a positively charged groove. The floor of the groove is composed of the H3 helices, and the sides are formed by the flanking loop regions (Figure 1a). The structure is very straight for the first 8 repeats, and then kinks between repeats 8 and 9 to form a pronounced cleft.

Despite a lack of significant sequence homology, the cadherin cytoplasmic domain, APC, and LEF/Tcf bind competitively to β-catenin (Hülsken et al., 1994; von Kries et al., 2000). The crystal structure of the β-catenin arm repeat domain complexed with a portion of *Xenopus* Tcf-3 (XTcf-3) suggested similarities in the binding of β-catenin to Tcf transcription factors and cadherins (Graham et al., 2000). Here we present the three-dimensional structures of both the unphosphorylated and phosphorylated E-cadherin cytoplasmic domains (E_{cyto}) complexed with β-catenin. These structures reveal how β-catenin uses the same surface to bind its various partners, and provides insights into the modulation of protein-protein interactions by phosphorylation.

Results and Discussion

Overall Structure of the E-Cadherin/β-Catenin Complex

Murine E-cadherin cytoplasmic domain, designated E_{cyto} (residues 577–728 of the mature E-cadherin sequence), and the proteolytically defined arm repeat domain of murine β-catenin (residues 134–671, referred to as "β-catenin" hereafter) (Huber et al., 1997) were prepared as described previously (Huber et al., 2001). The complex was crystallized using either unphosphorylated E_{cyto} or in vitro phosphorylated E_{cyto} (phos-E_{cyto}). The structures of both E_{cyto}/β-catenin and phos-E_{cyto}/β-catenin complexes were determined (Table 1). In each case, the crystals contain two copies in the asymmetric unit, providing four crystallographically independent views of the complex. The structure of β-catenin in these complexes is essentially the same as reported previously (Graham et al., 2000; Huber et al., 1997). The structure of β-catenin bound to either E-cadherin or XTcf-3 shows two significant differences relative to the unliganded

[1]Correspondence: bill.weis@stanford.edu

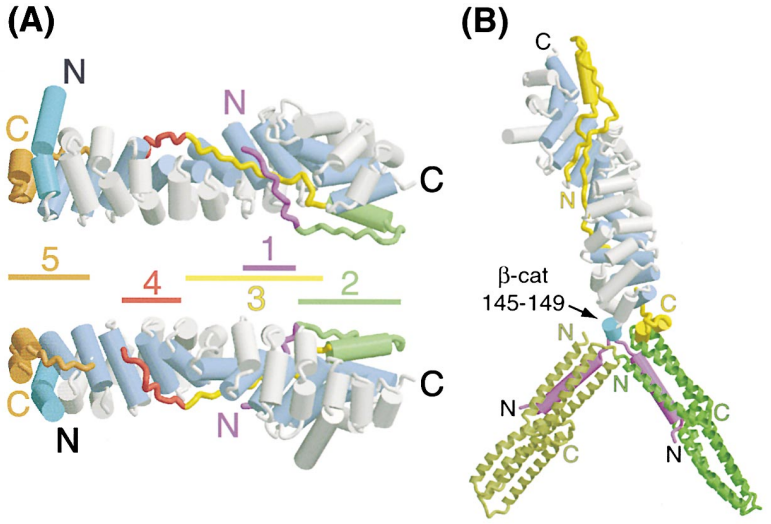

Figure 1. Overall Structure of the E_{cyto}/β-Catenin Complex

Cylinders represent α helices. The arm repeat region of β-catenin is shown in gray (H1, H2, and intervening loops) and blue (H3).

(A) Ribbon diagram of the complex. The single, kinked helix between β-catenin residues 134 and 161 is shown in cyan. The five regions of E-cadherin are shown in magenta (I), green (II), yellow (III), red (IV), and brown (V). The N and C terminus of each protein is marked.

(B) A hinge in the α-catenin/β-catenin interface. The βα-cat structure was superimposed on the corresponding β-catenin residues in the E_{cyto} (green) or XTcf-3 (olive green) complex using residues 146–149 of β-catenin (cyan). Residues 118–144 of β-catenin, as seen in the βα-cat structure, are shown in magenta. Residues 134–145 of β-catenin in the E_{cyto} or XTcf-3 complexes have been omitted. E-cadherin is shown in yellow. Note the clash of α-catenin with the E_{cyto} region V cap in the E_{cyto} complex.

structure. First, in some of the crystallographically independent copies, the previously disordered residues 134–149 of β-catenin are now visible as part of a continuous helix that runs between 134 and 161. Second, in both the E-cadherin and XTcf-3 complexes, the loop replacing the H1 helix of repeat 7 (Huber et al., 1997) adopts a conformation that is apparently stabilized by ligand binding.

The E_{cyto}/β-catenin interaction surface is extensive, spanning the entire length of the β-catenin arm repeat domain and involving the C-terminal 100 residues of the cadherin cytoplasmic domain. To facilitate description

Table 1. Crystallographic Data

	Unphosphorylated	Phosphorylated
Space group	C2	C2
a (Å)	180.8	168.6
b (Å)	134.2	85.3
c (Å)	94.2	115.1
β (°)	94.3	107.9
Data Collection Statistics		
Resolution range	30.–3.0 (3.11–3.0)	50.–2.0 (2.07–2.0)
No. measured reflections	109,516	287,321
No. unique reflections	44,525	101,570
% complete	98.5 (98.6)	96.7 (94.9)
% $> 3\sigma(I)$	74.7 (38.7)	74.1 (35.2)
R_{sym}[a]	0.079 (0.368)	0.040 (0.339)
Refinement Statistics		
R_{cryst}[b]	0.196	0.206
R_{free}[b]	0.242	0.245
No. protein atoms	8920	8515
No. solvent molecules	20	679
Bond length rmsd (Å)	0.007	0.007
Bond angle rmsd (°)	1.2	1.2
Ramachandran plot		
% in most favorable regions[c]	89.9	96.4
% in disallowed regions[c]	0.0	0.0
Average B value (Å^2)		
Protein	58.3	46.8
Solvent	30.4	49.0

Values in parentheses are for the highest resolution shell.

[a] $R_{sym} = \Sigma_h\Sigma_i|(I_i(h) - \langle I(h)\rangle|/\Sigma_h\Sigma_i I_i(h)$, where $I_i(h)$ is the I^{th} measurement of reflection h, and $\langle I(h)\rangle$ is the weighted mean of all measurements of h.

[b] $R = \Sigma_h||F_{obs}(h)| - |F_{calc}(h)||/\Sigma_h|F_{obs}(h)|$. R_{cryst} and R_{free} were calculated using the Working and Test reflection sets, respectively. The Test set comprises a randomly selected subset of the data (8.1% and 5.5% of unphosphorylated and phosphorylated data sets, respectively) that was not included in the refinement of the model. The Working Set contains the remaining reflections from the data set.

[c] As defined in PROCHECK.

of the complex, we divide the interactions into five regions, labeled I–V, ordered in the N- to C-terminal direction of the E-cadherin chain (Figure 1a). Region I (residues 628–638) starts as an extended polypeptide within the β-catenin groove at arm repeats 7–9, running parallel to the H3 helices and toward the β-catenin C terminus. Region II (residues 639–666) starts by running roughly parallel to the β-catenin superhelical axis before doubling back upon itself at the β-catenin C terminus, where it forms a helix that packs against arm repeats 12 and 11. Region III (residues 667–684) continues as an extended polypeptide that runs along the β-catenin groove toward its N terminus, passing underneath and interacting with region I. Region III contacts arm repeats 9–4. The chain turns at region IV (residues 685–694), which runs antiparallel to the H3 helices of repeats 4 and 3. The next three residues are disordered, and then region V (residues 698–723) continues toward the N terminus of the β-catenin groove and terminates in two short helices that cap exposed hydrophobic core residues at the N terminus of β-catenin. Approximately 6100 Å^2 of surface area is buried in the complex, with 2900 Å^2 contributed by β-catenin and 3200 Å^2 by E_{cyto}.

Region I is observed in two of the four independent copies of the structure. Regions II and III are observed in all four copies. Region IV is present only when E-cadherin is phosphorylated, and region V is observed in three of the four copies. E-cadherin residues 577–627, 695–697, and 724–728 are not observed in any of the independent structures. Although some of the binding regions appear to be more dynamic than others, data from previous studies show that most, if not all of these regions contribute to the affinity of the complex.

Regions I–III

E_{cyto} region I sits in the cleft formed by a kink in the β-catenin superhelix (Huber et al., 1997). Residues 631–633 cross over and interact with region III residues 674–676, forming a short pair of β strands. Region I also packs against region III Tyr673 and forms specific interactions with β-catenin repeats 8 and 9 (Figure 2a). Region II starts as a poorly ordered stretch from residues 639–652 that reverses direction at the C terminus of the arm repeats. E_{cyto} residues 653–666 then form an amphipathic helix that packs against repeats 12 and 11 (Figure 2b). β-catenin Tyr654 packs against the region II helix and forms a hydrogen bond with E_{cyto} Asp665. Transfection of cells with pp60$^{v\text{-}src}$ leads to disassembly of junctions and a gain-of-invasiveness phenotype associated with metastasizing cells (Behrens et al., 1993; Hamaguchi et al., 1993; Matsuyoshi et al., 1992; Takeda et al., 1995). Phosphorylation of Tyr654 by pp60$^{c\text{-}src}$ causes a 6-fold reduction in the affinity of β-catenin for E-cadherin, suggesting that tyrosine phosphorylation of β-catenin can modify junctional stability (Roura et al., 1999). Phosphorylation of Tyr654 likely causes E_{cyto} region II to dissociate from β-catenin because the phosphate group is too large to be accommodated in the interface, and would electrostatically repel E_{cyto} Asp665.

Region III starts with a sequence highly conserved among classical cadherins (E-cadherin residues 667–673) that binds within the β-catenin cleft (Figure 3a). The polypeptide backbone in this region adopts an unusual conformation that features a *cis*-proline at position 672 and extensive hydrogen bonding interactions with β-catenin Arg474. The chain continues along the β-catenin groove, with the extended region from E_{cyto} Asp674 through Ser684 forming part of a highly conserved "core" region essential for the E-cadherin/β-catenin interaction (Stappert and Kemler, 1994). E_{cyto} Asp674 and Glu682 form salt bridges with β-catenin Lys435 and Lys312, respectively, and Leu676, Leu677, Phe679, and Tyr681 form nonpolar contacts with β-catenin (Figure 3a). Mutation of either β-catenin Lys312 or Lys435 to glutamate abolishes binding to cadherins (Graham et al., 2000), implying that the region III interactions are essential.

The binding of the extended portion of region III is reminiscent of the binding of similarly extended NLS peptides to karyopherin α (Conti et al., 1998). In each case, asparagine side chains from the arm repeats are used to satisfy the hydrogen bonding potential of the extended polypeptide backbone, supporting the hypothesis that these residues are conserved for this purpose (Conti et al., 1998). β-catenin utilizes Asn387, Asn426, and His470 in the binding of E-cadherin and XTcf-3 (Graham et al., 2000). These residues are located in arm repeats 6, 7, and 8 and lie within the same turn of helix 3, a position occupied by asparagine throughout most of the karyopherin α repeats (Conti et al., 1998; Fontes et al., 2000) (Figure 3b). Asparagines are present in this position of the p120^{ctn} and APC arm repeats (Figure 3b), and it is likely that these proteins also use asparagines to recognize extended ligands.

Phosphorylation-Induced Structure in Region IV

The region between E-cadherin residues 684 and 699 contains several serine residues in consensus positions for casein kinase II (CKII)- and GSK-3β-mediated phosphorylation (Figure 4). Substituting these serine residues with alanine reduces β-catenin/E-cadherin complex formation and diminishes cell-cell adhesion (Lickert et al., 2000; Stappert and Kemler, 1994). E_{cyto} residues 685–697 are not visible in the unphosphorylated complex structures, suggesting that phosphorylation is required for their association with β-catenin. E_{cyto} was treated with CKII, or CKII and GSK-3β, under conditions that produced a heterogeneous pool of phosphorylated E_{cyto} with 0–6 phosphates. A limiting amount of β-catenin was added and E_{cyto}/β-catenin complex separated from unbound E_{cyto}. Analysis of the unbound E_{cyto} pool revealed significant depletion of the 5- and 6-phospho species, whereas the bound E_{cyto} comprised the 4-, 5-, and 6-phospho species (Figure 5a).

In the crystal structure of the phos-E_{cyto}/β-catenin complex, E-cadherin residues 685–694 are visible, with ordered phosphate groups present on Ser684, Ser686, and Ser692 (Figure 5b). E_{cyto} Ser684 is visible in the unphosphorylated complex, but does not interact with β-catenin. When phosphorylated, it interacts with both β-catenin and phos-E_{cyto} phosphoserine 686 (pSer686) through water molecules. Phos-E_{cyto} pSer686 forms a salt bridge with β-catenin Arg342 and water-mediated contacts with β-catenin Trp338 and Asn380. pSer692, which lies within the invariant E-cadherin sequence Ser690-Leu-Ser-Ser-Leu694, forms hydrogen bonds

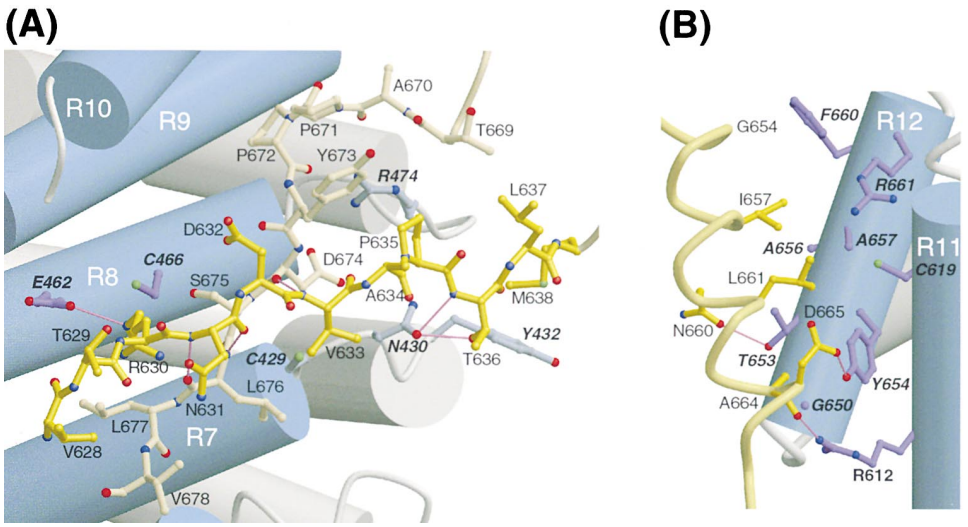

Figure 2. Interaction Regions I and II

β-catenin is represented as in Figure 1, and the arm repeats are marked "R." Residues of β-catenin are labeled in bold italics, and residues of E-cadherin in plain text. Oxygen, nitrogen, and sulfur are shown as red, blue, and green spheres, respectively. Individual side chains of β-catenin are shown in purple (H3) or gray (others). In this and Figures 3, 5, and 6, only those β-catenin residues that form direct contacts with E-cadherin are shown. E-cadherin is shown with yellow bonds. Hydrogen bonds and salt bridges are shown as thin pink lines. (A) Region I. Nearby region III residues are shown in light yellow. (B) Region II.

with Tyr333 and Lys335 when phosphorylated (Figure 5b). The leucines of this sequence pack against nonpolar patches on the surface of β-catenin (Figure 5b). The dependence of binding on phosphorylation may reflect the need to lock Lys335 in an extended conformation that contributes to the formation of the hydrophobic pocket.

Only E-cadherin Ser684 is a consensus CKII site, whereas Ser686 and Ser692, which directly contact β-catenin, are consensus GSK-3β sites (Figure 4). Consensus sites for phosphorylation are not strict, and CKII presumably also phosphorylates the GSK-3β sites, albeit with low efficiency. Thus, it is likely that only the more heavily phosphorylated fractions (Figure 5a) contain phosphoserines in the GSK-3β consensus positions, which would explain the preferential binding of these species to β-catenin. Although the kinases responsible for phosphorylating cadherins in vivo are not known definitively, it is clear that phosphorylation of these serines leads to specific phosphoserine interactions with β-catenin and the binding of otherwise disordered flanking cadherin sequences.

A Hydrophobic Cap in Region V

The C terminus of E_{cyto} forms two antiparallel helices that pack against otherwise exposed hydrophobic core residues from the first arm repeat, forming a "cap" at this end of the arm repeat domain (Figure 5c). The hydrophobic surface presented by E-cadherin is formed from Leu708, Phe715, and Leu718, which are flanked by a number of aromatic residues and a methionine (Figure 5c). Removal of the N-terminal repeats from β-catenin substantially reduces the amount of E-cadherin coimmunoprecipitated with β-catenin (Hülsken et al., 1994), and deletion of the E-cadherin cap residues likewise reduces the interaction with β-catenin (Finnemann et al., 1997; Stappert and Kemler, 1994). In one copy of the unphosphorylated E_{cyto}/β-catenin complex, the cap is not visible. This portion of β-catenin is in a lattice contact, suggesting that the region V interaction is somewhat dynamic, and that lattice formation can compete for the cap binding site.

Sequestration of Cadherins from Degradation

Cadherins associate with β-catenin in the endoplasmic reticulum shortly after their synthesis, whereas uncomplexed cadherins are degraded (Hinck et al., 1994). The cytoplasmic tails of many type I and type II cadherins contain PEST sequences, which are motifs associated with rapid protein turnover (Rechsteiner and Rogers, 1996). These sequences overlap or encompass the β-catenin binding region of E-cadherin and were hypothesized to be sequestered by β-catenin, thereby protecting bound cadherins from degradation (Huber et al., 2001). In this way, cadherins that are not bound to β-catenin would be turned over rapidly, while cadherins bound to β-catenin could proceed to the cell surface to participate in adherens junctions. Structurally, the predicted cadherin PEST sequences start just before the beginning of region III and continue through to the middle of the region V cap structure. The region IV sequence (Figure 4) is contained within every predicted PEST sequence and was noted to feature two characteristics of synthetic signals that target proteins to the ubiquitin-proteasome pathway in *S. cerevisiae*: a high content of serine and threonine residues and the sequence motif, (bulky hydrophobic)-(Ser/Thr)-(Ser/Thr)-(bulky hydrophobic) (Huber et al., 2001). Thus, phosphorylation-dependent binding of the Leu-Ser-Ser-Leu sequence in region IV may be important in sequestering cadherin from the degradation machinery.

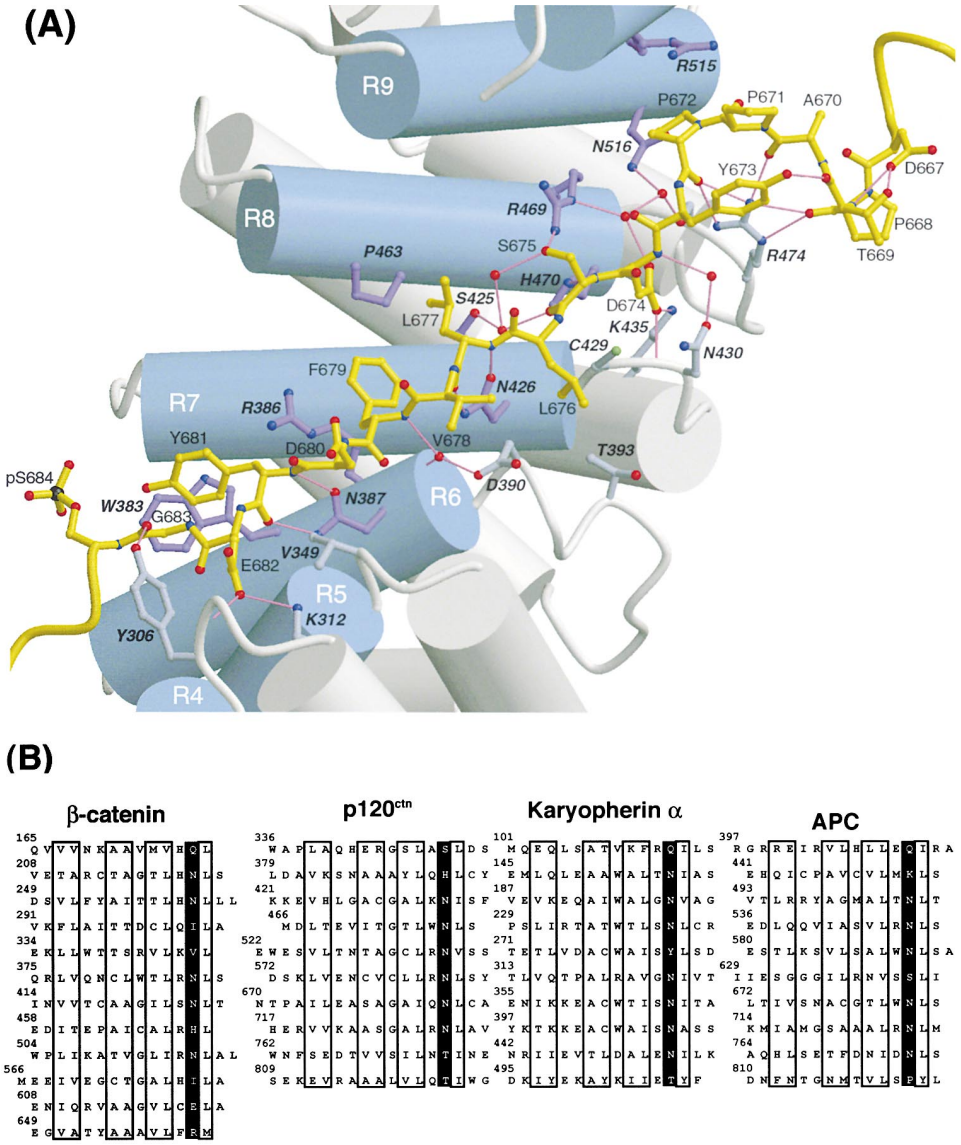

Figure 3. The Extended Region III

(A) Interactions of region III, colored as in figure 2. (B) Alignment of the H3 helices from murine β-catenin, murine p120^{ctn}, yeast karyopherin α, and murine APC arm repeat domains. The position of the conserved asparagines responsible for recognizing the backbone of extended peptides is highlighted in black. Conserved hydrophobic positions (Conti et al., 1998; Huber et al., 1997) are boxed. The starting residue number for each sequence is indicated.

Comparison with XTcf-3 Binding

Overall, the E_{cyto}/β-catenin and XTcf-3/β-catenin complexes are remarkably similar, with the XTcf-3 interactions essentially a subset of the E_{cyto} interactions (Figure 6a). E_{cyto} region I enters the β-catenin cleft along the wall formed by arm repeats 7–9. XTcf-3 residues 2–15 enter the β-catenin cleft from the same direction, but run along the opposite wall of the cleft. E_{cyto} then exits into region II, which extends the interactions into arm repeats 11 and 12 before entering the extended region III, whereas XTcf-3 enters a hairpin turn that begins the XTcf-3 extended binding region (Graham et al., 2000). At the start of region III, E_{cyto} features a "crown" of backbone carbonyl oxygens that interact with β-catenin Arg474 (Figure 3a); this arginine interacts with both main-chain and side-chain functionalities of the XTcf-3 hairpin (Graham et al., 2000).

Based on the XTcf-3 complex structure, it was proposed that XTcf-3 residues 16–24, which bind in an extended conformation, were homologous to E-cadherin residues 674–682, a region known to interact with β-catenin (Graham et al., 2000). Indeed, the structures of these ligands are strikingly similar in this region (region III, Figure 6b). Interestingly, E-cadherin pSer684 and pSer686 are in structural register with XTcf-3 Glu26 and Glu28 (Figure 6b), raising the possibility that XTcf-3 mimics the phosphorylated cadherin. However, in the XTcf-3 complex structure, these residues are present in a highly unusual backbone configuration and do not interact with β-catenin.

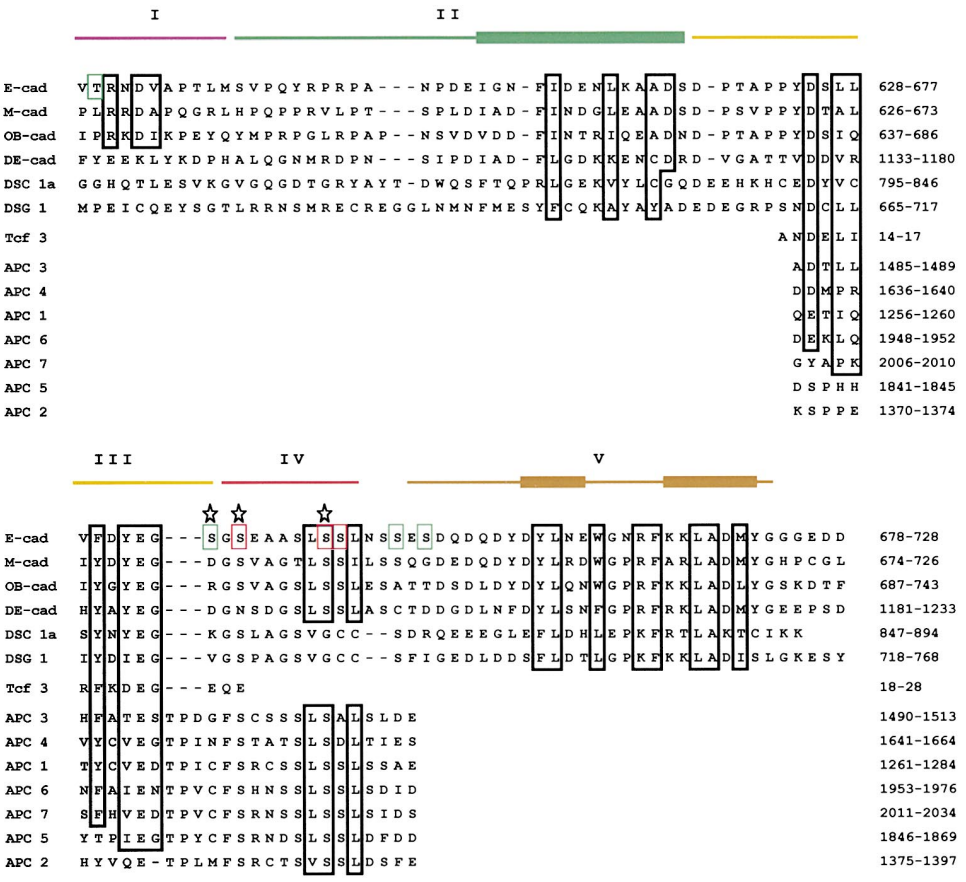

Figure 4. Sequence Alignments

The cytoplasmic domains of representative cadherins from different classes (Nollet et al., 2000) are aligned with that of the classical/type-I murine E- cadherin: M-cadherin, a classical/type-I cadherin; OB-cadherin, a type-II cadherin; *Drosophila* E-cadherin, a cadherin-related molecule; desmocollin 1a and desmoglein 1, two desmosomal cadherins. Residue ranges are shown on the right. The portion of XTcf-3 corresponding to the structurally related region III of E-cadherin is shown, as well as the 20-mer repeats of APC. The five regions of the E-cadherin cytoplasmic domain are indicated with colored bars corresponding to Figure 1A; the thickened rectangles correspond to helices. Key conserved residues are boxed. The stars mark the three phosphoserines observed in the present structure. Consensus sites for GSK-3β (SxxxS/T) and CKII (SxxD/E) phosphorylation are boxed in red and green, respectively, on the E-cadherin sequence.

Following the extended region, E_{cyto} and XTcf-3 interact with essentially the same β-catenin residues, but do so using different secondary structures. In a remarkable case of molecular mimicry, Leu41 and Leu48 on one face of an amphipathic XTcf-3 helix occupy the same positions as Leu691 and Leu694 from the extended region IV of phosphorylated E-cadherin (Figure 6c). In addition, the γ carbons of XTcf-3 Val44, the third residue on this face of the XTcf-3 helix, occupy similar positions as two water molecules in the E-cadherin complex (Figure 6c). Finally, although the positions of the side chains differ, the interaction of E-cadherin pSer692 with β-catenin Lys335 is equivalent to the salt bridge between this lysine and Asp40 at the start of the XTcf-3 helix (Figure 6c).

α-Catenin Binding and Adherens Junction Structure

Amino acids 118–149 of β-catenin comprise the α-catenin binding site (Aberle et al., 1996). We have previously shown that a chimeric protein (βα-cat), consisting of β-catenin residues 118–149 fused to the β-catenin binding domain of α-catenin by a polyglycine linker, faithfully mimics the interaction of α- and β-catenins (Pokutta and Weis, 2000). In the βα-cat structure, β-catenin residues 118–141 form an amphipathic helix that completes a four helix bundle with α-catenin. Residues 143–145 adopt an extended conformation, and residues 146–149 form an additional turn of helix oriented in a different direction from that of 118–141.

The N terminus of the proteolytically defined β-catenin arm repeat domain, comprising residues 134–149, was not visible in structures of the uncomplexed protein (Huber et al., 1997), but is observed in the unphosphorylated E_{cyto} complexes and in one copy of the XTcf-3 complex (Graham et al., 2000). In each of these structures, residues 134–160 form a kinked, but continuous, helix (Figure 1a) that is part of a lattice contact. It is highly unlikely that this extended helix reflects the structure of β-catenin in the β-catenin/α-catenin complex as recently proposed (Graham et al., 2000). Inspection of the βα-cat structure reveals that the N-terminal β-catenin helix cannot continue past residue 142 because doing so would introduce steric clashes between β-catenin

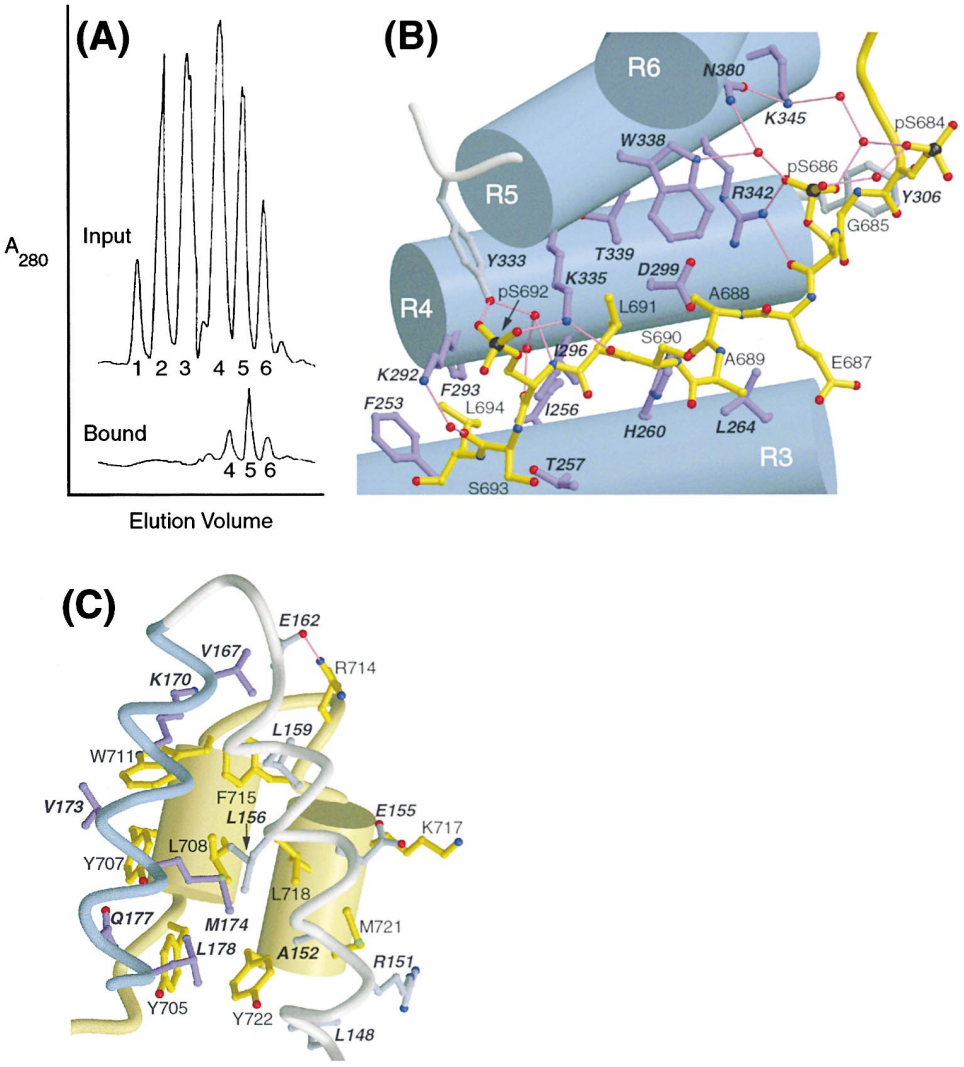

Figure 5. Interaction Regions IV and V

(A) Anion-exchange column analysis of E-cadherin treated with CKII as described in Experimental Procedures, before binding to β-catenin ("input") and after elution from β-catenin ("bound"). Numbers under each peak denote the number of phosphates bound to E-cadherin, as determined by mass spectrometry. (B) Structure of phosphorylated E-cadherin region IV bound to β-catenin. (C) Interaction of the region V hydrophobic cap with the N-terminal arm repeats of β-catenin. Parts (B) and (C) are colored as in Figure 2; phosphorous is represented as a black sphere.

Gln143 and α-catenin residues Phe111 and Arg121. This implies that β-catenin residues 143–145 must be nonhelical when bound to α-catenin. Thus, it is likely that in the β-catenin/E-cadherin and β-catenin/XTcf-3 complexes, only residues 146–149 adopt the conformation and orientation with respect to the arm repeat domain that exists in the complex with α-catenin. Superimposing β-catenin 146–149 from the βα-cat structure onto the corresponding residues of β-catenin in either of its complexes with E_{cyto} or XTcf-3, and using the β-catenin 118–145 conformation seen in βα-cat structure, yields a model free of steric clashes between α- and β-catenin (Figure 1b).

Comparison of the E-cadherin and XTcf-3 complexes reveals that the helical regions of β-catenin preceding Thr150 are rotated with respect to one another by 100° about the helix axis. The presence of proline in the middle of a helix is associated with hinge motions (Gerstein et al., 1994), and the difference observed here presumably reflects motion about a hinge created by β-catenin Pro154. When βα-cat residues 146–149 are superimposed onto the corresponding residues of the E_{cyto} or XTcf-3 complexes, the different helix registers give rise to substantially different α-catenin positions (Figure 1b). In the case of the E_{cyto} complex, superposition produces a steric clash with the E_{cyto} region V cap (Figure 1b). Thus, the presence of the E_{cyto} cap may restrict hinge motion in β-catenin. The dynamics of the region V/β-catenin interaction would then have a role in determining the relative orientations of α- and β-catenin.

The higher-order structure of the adherens junction is not evident from the E_{cyto}/β-catenin complex and the βα-cat (Pokutta and Weis, 2000) structure. The 51 membrane-proximal amino acids of E_{cyto} are not observed in

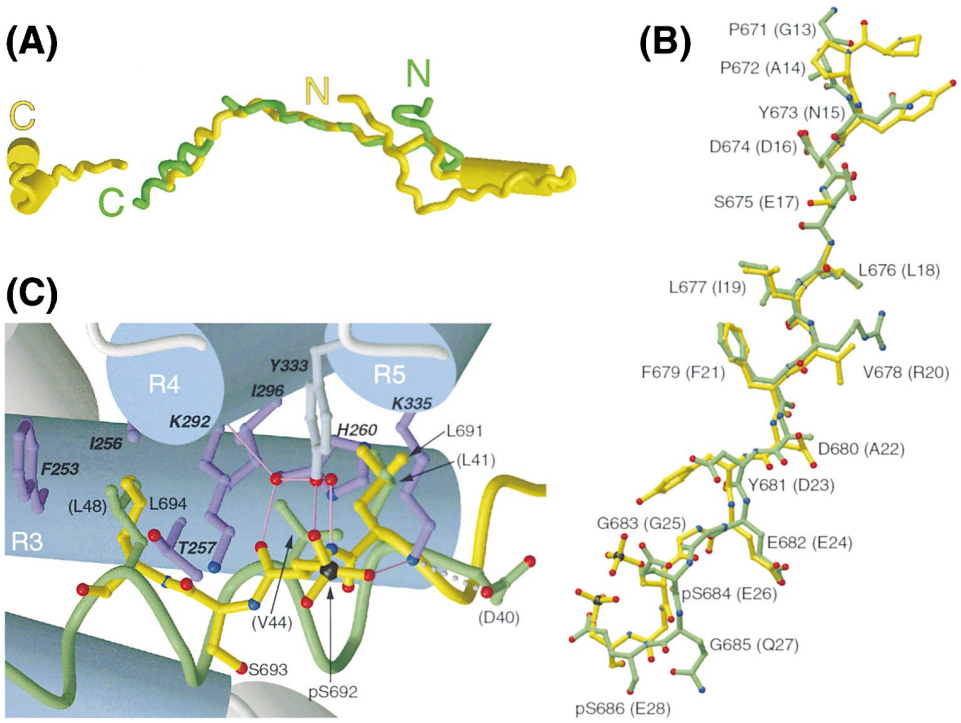

Figure 6. Comparison of E_{cyto} and XTcf-3 Binding to β-Catenin

E-cadherin is shown in yellow and XTcf-3 in green. (A) Overall comparison of E-cadherin and XTcf-3 bound to β-catenin. (B) Overlay of the extended region III of E-cadherin with the corresponding portion of XTcf-3. (C) Comparison of the phosphorylated region IV interaction. Figure colored as in figures 2 and 4.

the E_{cyto}/β-catenin complexes, so no conclusions can be drawn regarding the relative disposition of β-catenin and the cell membrane. Lateral dimerization of cadherins mediated by the extracellular domain is believed to modulate adhesive strength (Brieher et al., 1996; Chitaev and Troyanovsky, 1998; Takeda et al., 1999; Yap et al., 1997b, 1998). The interfaces between neighboring E-cadherin/β-catenin complexes differ in the two crystal forms, and we see no evidence for dimerization mediated by either the cadherin cytoplasmic domain or β-catenin, consistent with the observation that the E_{cyto}/β-catenin complex is a 1:1 heterodimer in solution (Huber et al., 2001).

Binding of Plakoglobin to Classical and Desmosomal Cadherins

Plakoglobin, a component of adherens junctions and desmosomes, and β-catenin are closely related, sharing 80% sequence identity within their arm repeat domains. Plakoglobin can bind the cytoplasmic domains of the desmosomal cadherins, desmogleins, and desmocollins, as well as classical cadherins. The β-catenin residues that interact with E-cadherin are conserved in plakoglobin, explaining the ability of the latter to bind to classical cadherins.

An alignment of desmoglein and desmocollin sequences with E-cadherin shows that many of the observed E-cadherin/β-catenin interactions are likely to be conserved in plakoglobin/desmosomal cadherin complexes (Figure 4). Region III and region V contacts appear to be well conserved among all desmosomal cadherins. The Ser-Leu-Ser-Ser-Leu sequence characteristic of region IV in classical cadherins is absent, although a number of hydrophobic residues that might form similar contacts are conserved among desmosomal cadherins. Plakoglobin arm repeats 11–12 are needed to bind desmocollins but not desmogleins (Witcher et al., 1996). β-catenin arm repeats 11–12 interact with the E-cadherin region II amphipathic helix residues Ile657, Leu661, and Ala664. These positions are conservatively substituted in desmocollins but not desmogleins, possibly explaining their differing dependencies on plakoglobin arm repeats 11–12. The conservation of E-cadherin/β–catenin contact residues in the desmosomal cadherins may also explain why the β-catenin arm repeat domain, which does not normally associate with desmosomal cadherins in vivo, is capable of binding to desmosomal cadherins under some circumstances (Norvell and Green, 1998; Ruiz et al., 1996; Wahl et al., 2000).

The region V cap structure appears to be more important in plakoglobin/desmosomal cadherin interactions than in β-catenin/classical cadherin interactions. Deletion of plakoglobin arm repeats 1–3 eliminates desmosomal cadherin binding (Chitaev et al., 1998; Witcher et al., 1996), whereas a similar β-catenin deletion mutant significantly compromises but fails to eliminate E-cadherin binding (Stappert and Kemler, 1994). The presence of a desmosomal cadherin cap structure is supported by the strong conservation of region V hydrophobic residues. The central E-cadherin cap residues, Leu708, Phe715, and Leu718, are present in all desmosomal cadherins. Several of the hydrophobic residues in the

outer rim of the cap structure are substituted with amino acids of increased hydrophobicity (Figure 4), which may make it more energetically favorable to bury the desmosomal cap residues in an interface with plakoglobin.

α-Catenin interacts with either β-catenin or plakoglobin in adherens junctions, but it is excluded from desmosomes, where plakoglobin is bound to desmosomal cadherins and desmoplakin. Mutagenesis studies suggest that the plakoglobin binding sites for α-catenin and desmosomal cadherins overlap (Troyanovsky et al., 1996; Witcher et al., 1996), providing a simple explanation for the absence of α-catenin in desmosomes. Mutating hydrophobic residues in the α-catenin binding helix of plakoglobin eliminates α-catenin and desmoglein binding (Chitaev et al., 1998). These data indicate that there are additional interactions in plakoglobin/desmosomal cadherin complexes beyond those observed in the β-catenin/E-cadherin complex. We suggest that the more hydrophobic nature of the desmosomal cap residues creates a surface that can interact with the amphipathic α-catenin binding helix, preventing plakoglobin from binding to α-catenin.

Implications for APC Binding

APC binds to β-catenin using one or more of its three 15- and seven 20-amino acid repeats (Rubinfeld et al., 1993; Su et al., 1993). The 15- and 20-mer repeats share significant sequence homology in their first 12 residues (referred to here as the "core homology region"), and mutagenesis suggests that they have distinct but overlapping binding sites on β-catenin (von Kries et al., 2000). The striking similarity in the interactions of E_{cyto} and XTcf-3 with β-catenin raises the question of whether APC binds in the same manner. The Leu691-Ser-Ser-Leu694 motif of E-cadherin region IV, which only binds to β-catenin when Ser692 is phosphorylated (Figure 5b), is conserved in the APC 20-mer repeats (Figure 4). Using this homology to set the register of the E-cadherin and APC sequences, E-cadherin pSer686, which binds directly to β-catenin, aligns with an invariant serine present in the APC 15- and 20-mer repeats as a conserved consensus GSK-3β phosphorylation site (Figure 4). Phosphorylation of APC by GSK-3β enhances APC/β-catenin complex formation (Rubinfeld et al., 1996). Furthermore, the first serine of the LSSL motif (Ser692 of E-cadherin) is a consensus GSK-3β site in APC repeats 1 and 2. These observations suggest that phosphorylated APC 20-mer repeats bind to β-catenin in a manner similar to the phosphorylated E-cadherin region IV. This structural alignment places the core homology region, which precedes the 20-mer Leu-Ser-Ser-Leu motif (Figure 4), in the vicinity of β-catenin arm repeats 5 and 6. This is consistent with the observation that mutations in this portion of β-catenin affect binding of the APC 15- and 20-mer repeats. A noteworthy difference between the APC and E-cadherin sequences is that a glycine precedes the pSer686 position in cadherins, whereas an invariant aromatic residue occupies this position in the APC repeats. Modeling suggests that the aromatic ring could be accommodated at this position by packing against Tyr306 of β-catenin.

In several of the APC 20-mer repeats, the sequence N-terminal to the core homology region displays detectable homology to the extended region III sequence of E-cadherin and XTcf-3 (Figure 4). This raises the possibility that at least some of the APC 20-mer repeats can mimic E-cadherin and XTcf-3 in this region. The 20-mer repeats 3 and 4 present the best match (Figure 4). It has been noted that the conserved Leu-Ser-Ser-Leu region in these two repeats is part of a sequence (Leu-x-x-Leu-x-ϕ, ϕ = Leu, Ile, Met, or Val) needed for APC to export β-catenin from the nucleus, a property associated with tumor suppression (Rosin-Arbesfeld et al., 2000). It is interesting to speculate that binding of 20-mer repeats 3 and 4 to β-catenin is determined by the extended and the core homology regions, leaving the Leu-x-x-Leu-x-ϕ sequence unbound and available for the nuclear export function.

Conclusions

The cadherin cytoplasmic domain is not structured in the absence of β-catenin (Huber et al., 2001), and binds in an extended conformation that forms a large interface with β-catenin. This mode of binding may allow for degrees of regulation that would be impossible for an interaction involving a well-structured ligand. The surface of such a ligand is presented on a relatively rigid scaffold, and local changes can therefore affect the entire interface between the two proteins. In contrast, the interface between a ligand that is unstructured in its unbound state and its partner can be altered locally without affecting the rest of the interface. In this manner, posttranslational modifications like phosphorylation can modulate the interaction in a graded fashion rather than serving as a simple on/off switch.

The armadillo repeat domain architecture complements the binding of extended polypeptides by providing a large surface-to-volume ratio and elongated interaction surface. Multiple, quasi-independent interactions provide the possibility of having a minimal "core" binding region while allowing other interactions to be more dynamic. Separate binding regions can be regulated independently, enabling combinatorial regulation of the interaction and the integration of multiple input signals. In the case of E-cadherin, the extended region III appears to be absolutely required for the interaction with β-catenin, as destabilizing the interface by mutation of either β-catenin Lys435 or Lys312 to glutamate destroys binding (Graham et al., 2000). In contrast, the enhanced binding of phosphorylated E-cadherin (region IV) (Lickert et al., 2000) (Figure 5a) or the decreased binding of E-cadherin upon phosphorylation of β-catenin Tyr654 (region II) (Roura et al., 1999) demonstrate that the overall affinity can be modulated without completely eliminating the interaction of these two proteins. An extended interface may also make the system somewhat resistant to mutations; for example, none of the 18 β-catenin alanine mutations reported by von Kries et al. (2000) eliminates binding to E-cadherin (J. von Kries and W. Birchmeier, personal communication). Combined, these features create a robust interface subject to regulation, which is likely to be important in determining the mechanical properties and dynamics of subcellular assemblies such as the adherens junction.

Experimental Procedures

Preparation of β-Catenin/E-Cadherin Complexes and E_{cyto} Phosphorylation

Full-length murine β-catenin, the β-catenin arm repeat domain, and the cytoplasmic domain of murine E-cadherin were expressed in *E. coli* and purified as described previously (Huber et al., 2001). Initial E_{cyto} phosphorylation reactions utilized recombinant human CKII (New England BioLabs) and rabbit GSK-3β (Sigma). E_{cyto} was treated for 3 hr with recombinant CKII (New England BioLabs) using the manufacturer's suggested reaction conditions. GSK-3β was then added and the reaction continued for 6 hr. Reactions were stopped by flash-freezing in liquid nitrogen. Anion exchange chromatography (MonoQ, Pharmacia) of the products yielded 7 peaks as measured by absorbance at 280 nm, which were analyzed by mass spectrometry. Similar phosphorylation profiles were produced with CKII alone.

The E_{cyto} mixture used to test the relative β-catenin binding affinities of the various phosphorylated species was produced using CKII only. Parallel reactions, one with limiting ATP and the other with excess ATP, produced mixtures with low and high amounts of phosphorylation, respectively. The reactions were stopped by adding apyrase, and combined to produce a mixture containing roughly equal amounts of E_{cyto} modified with different numbers of phosphates. This mixture was divided equally, with one aliquot added to a limiting amount of full-length β-catenin and the other used as a control. Gel filtration chromatography (S200, Pharmacia) was used to separate free and bound E_{cyto}. The unbound fraction was separated into its component phosphorylated species by MonoQ chromatography, and the resulting peaks integrated by weighing the peaks cut out of the absorbance trace. The control mixture was also analyzed by this method. This analysis revealed approximately 30% depletion of the 5- and 6-phospho species from the input mixture. The bound E_{cyto} was dissociated from β-catenin by vacuum evaporation of the pooled complex fractions obtained from the S200 column to near dryness, followed by dilution of the concentrate into 8 M urea, 400 mM glycine pH 2.5, incubation at 50°C for 30 min, and injection onto an S200 column equilibrated with Tris-HCl, pH 8.0, 8 M urea, and 150 mM NaCl. The resulting peak of dissociated phospho-E_{cyto} was separated into its component species on a MonoQ column and the peaks identified by mass spectrometry.

Preparative E_{cyto} phosphorylation reactions utilized CKII alone with reaction conditions optimized to favor production of the more heavily phosphorylated species, which were purified by MonoQ chromatography. Unphosphorylated or phosphorylated E_{cyto} was added at 10% molar excess to the arm repeat domain of β-catenin, and the complex concentrated without further purification to 5–10 mg/ml in 10 mM Tris-HCl, pH 8.5, 25 mM NaCl, and 2 mM dithiothreitol for crystallization.

Crystallization and Structure Determination

All crystals were grown at 20°C using vapor diffusion with hanging drops comprising equal volumes of protein complex and well solutions. Crystals of the unphosphorylated E_{cyto}/β-catenin complex were grown from 5–10 mg/ml protein solution mixed with reservoir containing 0.1% polyethyleneimine, pH 8.5, 200 mM Tris-HCl, pH 7.5, and 6% (v/v) isopropanol. Ethylene glycol (25%) was used as a cryoprotectant. Diffraction data (Table 1) were measured at the Stanford Synchrotron Radiation Laboratory (SSRL) beamline 9–2 (λ = 1.03 Å). The structure was solved by molecular replacement in AMORE (Navaza and Saludjian, 1997), using the ligand-free β-catenin structure (Huber et al., 1997) (Protein Data Bank ID code 2bct) as a search model. The model was refined in CNS using a maximum likelihood target and all data between 30 and 3.0 Å. Refinement statistics are shown in Table 1.

Crystals of the phospho-E_{cyto}/β-catenin complex were grown from 5–10 mg/ml protein stocks mixed with reservoir solutions containing 13.5% (w/v) polyethylene glycol monomethylether 5000, 200 mM Tris-HCl, pH 8.0, and 1.1 M NaCl. The data used for molecular replacement were measured to 2.7 Å measured on an RAXIS-IIc imaging plate detector mounted on a rotating anode source. The high resolution data used for refinement were measured at SSRL beamline 9–2 (λ = 0.98 Å) (Table 1) from a crystal frozen in Paratone-N (Exxon) for data collection. The structure was solved by molecular replacement in CNS (Brünger et al., 1998), using the uncomplexed β-catenin structure (Huber et al., 1997) (Protein Data Bank ID code 2bct) as a search model. The model was refined in CNS using a maximum likelihood target and all data between 50 and 2.0 Å. Refinement statistics are shown in Table 1.

Although region IV is present in both copies of the phosphorylated complex crystallized in 1.1 M NaCl, phosphates were visible on serines 684, 686, and 692 in one copy, whereas phosphate was seen only on Ser692 in the other. This suggested that the high concentration of NaCl present in the crystallization conditions might interfere with binding of the phosphates, and that perhaps other regions did not bind under these conditions. Therefore, a crystal of the phos-E_{cyto}/β-catenin complex was adapted into 150 mM NaCl by serial transfer into synthetic mother liquor containing 80% of the previous step's NaCl concentration. Data (not shown) were measured to 2.85 Å resolution on an RAXIS-IIc imaging plate detector mounted on a rotating anode x-ray generator, and the model partially refined. Phosphates are visible on serines 684, 686, and 692 in both copies of the low-salt complex, but there are no other differences in structure, so the interactions are described based on the 1.1 M NaCl, 2.0 Å structure.

Sequence Alignments

An initial alignment of three relatively divergent cadherin cytoplasmic domain sequences, two type-I and one type-II (Nollet et al., 2000), was performed with ClustalW (http://dot.imgen.bcm.tmc.edu) (Jeanmougin et al., 1998), then edited by hand. XTcf-3 was aligned using the known structures. The APC 20-mer repeats were aligned by hand using the conserved LSSL sequence motif to set the sequence register. Genbank accession numbers are: murine E-cadherin (Cad-1), X06115; human M-cadherin (Cad-15) D83542; human OB-cadherin (Cad-11) L34056; *Drosophila* DE-cadherin (D28749); human desmocollin 1a (AF293358); human desmoglein 1 (AF097935); *Xenopus* Tcf-3 (X99308); human APC (NM_000038).

Putative armadillo repeat domain sequences from murine $p120^{ctn}$ (GenBank accession number Z17804) and murine APC (M88127) were submitted to the 3D-PSSM Web Server V 2.5.1 (http://www.bmm.icnet.uk/~3dpssm/) (Kelly et al., 2000). In each case, the arm repeat domain structures from murine β-catenin (PDB code 2bct) and *S. cerevisiae* karyopherin α (Protein Data Bank ID code 1bk5) were returned as two of the highest scoring templates. H1, H2, and H3 helices were assigned using the predicted secondary structure of the query sequences as well as consistencies in the alignments with the two known structures. H3 helices were aligned according to structure-based consensus motifs (Conti et al., 1998; Huber et al., 1997).

Acknowledgments

We thank S. Fridman for technical assistance and A. May, S. Pokutta, and K. Spink for discussions and comments on the manuscript. We are grateful to M. Bienz for discussions, J. von Kries and W. Birchmeier for communicating unpublished results, and W. Xu for the XTcf-3/β-catenin complex coordinates. Some of this work is based upon research at SSRL, which is funded by the Department of Energy (BES, BER) and the National Institutes of Health (NCRR, NIGMS). This work was supported by grant GM56169 from the National Institutes of Health.

Received February 9, 2001; revised March 26, 2001.

References

Aberle, H., Schwartz, H., Hoschuetzky, H., and Kemler, R. (1996). Single amino acid substitutions in proteins of the *armadillo* gene family abolish their binding to α-catenin. J. Biol. Chem. *271*, 1520–1526.

Aberle, H., Bauer, A., Stappert, J., Kispert, A., and Kemler, R. (1997). β-catenin is a target for the ubiquitin-proteasome pathway. EMBO J. *16*, 3797–3804.

Behrens, J., Vakaet, L., Friis, R., Winterhager, E., van Roy, F., Mareel, M.M., and Birchmeier, W. (1993). Loss of epithelial differentiation and gain of invasiveness correlates with tyrosine phosphorylation

of the E-cadherin/β-catenin complex in cells transformed with a temperature-sensitive v-*src* gene. J. Cell Biol. *120*, 757–766.

Behrens, J., von Kries, J.P., Kühl, M., Bruhn, L., Wedlich, D., Grosschedl, R., and Birchmeier, W. (1996). Functional interaction of β-catenin with the transcription factor LEF-1. Nature *382*, 638–642.

Behrens, J., Jerchow, B.-A., Würtele, M., Grimm, J., Asbrand, C., Wirtz, R., Kühl, M., Wedlich, D., and Birchmeier, W. (1998). Functional interaction of an Axin homolog, conductin, with β-catenin, APC, and GSK3β. Science *280*, 596–599.

Brieher, W.M., Yap, A.S., and Gumbiner, B.M. (1996). Lateral dimerization is required for the homophilic binding activity of C-cadherin. J. Cell Biol. *135*, 487–496.

Brünger, A.T., Adams, P.D., Clore, G.M., Gros, P., Grosse-Kunstleve, R.W., Jiang, J.-S., Kuszewski, J., Nilges, M., Pannu, N.S., Read, R.J., et al. (1998). Crystallography and NMR System (CNS): a new software system for macromolecular structure determination. Acta Cryst. *D54*, 905–921.

Chitaev, N.A., and Troyanovsky, S.M. (1998). Adhesive but not lateral E-cadherin complexes require calcium and catenins for their formation. J. Cell Biol. *142*, 837–846.

Chitaev, N.A., Averbakh, A.Z., Troyanovsky, R.B., and Troyanovsky, S.M. (1998). Molecular organization of the desmoglein-plakoglobin complex. J. Cell Sci. *111*, 1941–1949.

Conti, E., Uy, M., Leighton, L., Blobel, G., and Kuriyan, J. (1998). Crystallographic analysis of the recognition of a nuclear localization signal by the nuclear import factor karyopherin α. Cell *94*, 193–204.

Finnemann, S., Mitrik, I., Hess, M., Otto, G., and Wedlich, D. (1997). Uncoupling of XB/U-cadherin-catenin complex formation from its function in cell-cell adhesion. J. Biol. Chem. *272*, 11856–11862.

Fontes, M.R.M., Teh, T., and Kobe, B. (2000). Structural basis of recognition of monopartite and bipartite nuclear localization sequences by mammalian importin-α. J. Mol. Biol. *297*, 1183–1194.

Gerstein, M., Lesk, A.M., and Chothia, C. (1994). Structural mechanisms for domain movements in proteins. Biochemistry *33*, 6739–6749.

Graham, T.A., Weaver, C., Mao, F., Kimmelman, D., and Xu, W. (2000). Crystal structure of a β-catenin/Tcf complex. Cell *103*, 885–896.

Gumbiner, B.M. (2000). Regulation of cadherin adhesive activity. J. Cell Biol. *148*, 399–403.

Hamaguchi, M., Matsuyoshi, N., Ohnishi, Y., Gotoh, B., Takeichi, M., and Nagai, Y. (1993). p60v-*src* causes tyrosine phosphorylation and inactivation of the N-cadherin-catenin cell adhesion system. EMBO J. *12*, 307–314.

Hinck, L., Nathke, I.S., Papkoff, J., and Nelson, W.J. (1994). Dynamics of cadherin/catenin complex formation: novel protein interactions and pathways of complex assembly. J. Cell Biol. *125*, 1327–1340.

Huber, A.H., Nelson, W.J., and Weis, W.I. (1997). Three-dimensional structure of the armadillo repeat region of β-catenin. Cell *90*, 871–882.

Huber, A.H., Stewart, D.B., Laurents, D.V., Nelson, W.J., and Weis, W.I. (2001). The cadherin cytoplasmic domain is unstructured in the absence of β-catenin: a possible mechanism for regulating cadherin turnover. J. Biol. Chem. *276*, 12301–12309.

Hülsken, J., Birchmeier, W., and Behrens, J. (1994). E-cadherin and APC compete for the interaction with β-catenin and the cytoskeleton. J. Cell Biol. *127*, 2061–2069.

Ikeda, S., Kishida, S., Yamamoto, H., Murai, H., Koyama, S., and Kikuchi, A. (1998). Axin, a negative regulator of the Wnt signaling pathway, forms a complex with GSK-3β and β-catenin and promotes GSK-3β-depedent phosphorylation of β-catenin. EMBO J. *17*, 1371–1384.

Jeanmougin, F., Thompson, J.D., Gouy, M., Higgins, D.G., and Gibson, T.J. (1998). Multiple sequence alignment with Clustal X. Trends Biochem. Sci. *23*, 403–405.

Kelly, L.A., MacCallum, R.M., and Sternberg, M.J.E. (2000). Enhanced genome annotation using structural profiles in the program 3D-PSSM. J. Mol. Biol. *299*, 501–522.

Lickert, H., Bauer, A., Kemler, R., and Stappert, J. (2000). Casein Kinase II phosphorylation of E-cadherin increases E-cadherin/β-catenin interaction and strengthens cell-cell adhesion. J. Biol. Chem. *275*, 5090–5095.

Matsuyoshi, N., Hamaguchi, M., Taniguchi, S., Nagafuchi, A., Tsukita, S., and Takeichi, M. (1992). Cadherin-mediated cell-cell adhesion is perturbed by v-*src* tyrosine phosphorylation in metastatic fibroblasts. J. Cell Biol. *118*, 703–714.

Navaza, J., and Saludjian, P. (1997). AMoRe: an automated molecular replacement program package. Methods Enzymol. *276*, 581–594.

Nollet, F., Kools, P., and van Roy, F. (2000). Phylogenetic analysis of the cadherin superfamily allows identification of six major subfamilies besides several solitary members. J. Mol. Biol. *299*, 551–572.

Norvell, S.M., and Green, K.J. (1998). Contributions of extracellular and intracellular domains of full length and chimeric cadherin molecules to junction assembly in epithelial cells. J. Cell Sci. *111*, 1305–1318.

Orford, K., Crockett, C., Jensen, J.P., Weissman, A.M., and Byers, S.W. (1997). Serine phosphorylation-regulated ubiquitination and degradation of β-catenin. J. Biol. Chem. *272*, 24735–24738.

Pai, L.-M., Kirkpatrick, C., Blanton, J., Oda, H., Takeichi, M., and Peifer, M. (1996). *Drosophila* α-catenin and E-cadherin bind to distinct regions of *Drosophila* Armadillo. J. Biol. Chem. *271*, 32411–32420.

Pokutta, S., and Weis, W.I. (2000). Structure of the dimerization and β-catenin binding region of α-catenin. Mol. Cell *5*, 533–543.

Polakis, P. (2000). Wnt signaling and cancer. Genes Dev. *14*, 1837–1851.

Rechsteiner, M., and Rogers, S.W. (1996). PEST sequences and regulation by proteolysis. Trends Biochem. Sci. *21*, 267–271.

Rosin-Arbesfeld, R., Townsley, F., and Bienz, M. (2000). The APC tumour suppressor has a nuclear export function. Nature *406*, 1009–1012.

Roura, S., Miravet, S., Piedra, J., García de Herreros, A., and Dunach, M. (1999). Regulation of E-cadherin/catenin association by tyrosine phosphorylation. J. Biol. Chem. *274*, 36734–36740.

Rubinfeld, B., Souza, B., Albert, I., Müller, O., Chamberlain, S.H., Masiarz, F.R., Munemitsu, S., and Polakis, P. (1993). Association of the *APC* gene product with β-catenin. Science *262*, 1731–1734.

Rubinfeld, B., Souza, B., Albert, I., Munemitsu, S., and Polakis, P. (1995). The APC protein and E-cadherin form similar but independent complexes with α-catenin, β-catenin, and plakoglobin. J. Biol. Chem. *270*, 5549–5555.

Rubinfeld, B., Albert, I., Porfiri, E., Fiol, C., Munemitsu, S., and Polakis, P. (1996). Binding of GSK3β to the APC-β-catenin complex and regulation of complex assembly. Science *272*, 1023–1026.

Ruiz, P., Brinkmann, V., Ledermann, B., Behrend, M., Grund, C., Thalhammer, C., Vogel, F., Birchmeir, C., Günthert, U., Franke, W.W., and Birchmeier, W. (1996). Targeted mutation of plakoglobin in mice reveals essential functions of desmosomes in the embryonic heart. J. Cell Biol. *135*, 215–225.

Stappert, J., and Kemler, R. (1994). A short core region of E-cadherin is essential for catenin binding and is highly phosphorylated. Cell Adhesion Commun. *2*, 319–327.

Su, L.-K., Vogelstein, B., and Kinzler, K.W. (1993). Association of the APC tumor suppressor protein with catenins. Science *262*, 1734–1737.

Takeda, H., Nagafuchi, A., Yonemura, S., Tsukita, S., Behrens, J., Birchmeier, W., and Tsukita, S. (1995). V-src kinase shifts the cadherin-based cell adhesion from the strong to the weak state and β catenin is not required for the shift. J. Cell Biol. *131*, 1839–1847.

Takeda, H., Shimoyama, Y., Nagafuchi, A., and Hirohashi, S. (1999). E-cadherin functions as a *cis*-dimer at the cell-cell adhesive interface *in vivo*. Nat. Struct. Biol. *6*, 310–312.

Troyanovsky, R.B., Chitaev, N.A., and Troyanovsky, S.M. (1996). Cadherin binding sites of plakoglobin: localization, specificity and role in targeting to adhering junctions. J. Cell Sci. *109*, 3069–3078.

van de Wetering, M., Cavallo, R., Booijes, D., van Beest, M., van Es, J., Loureiro, J., Ypma, A., Hursh, D., Jones, T., Bejsovec, A., et al.

(1997). Armadillo coactivates transcription driven by the product of the Drosophila segment polarity gene *dTCF*. Cell *88*, 789–799.

von Kries, J.P., Winbeck, G., Asbrand, C., Schwarz-Romond, T., Sochnikova, N., Dell'Oro, A., Behrens, J., and Birchmeier, W. (2000). Hot spots in β-catenin for interactions with LEF-1, conductin, and APC. Nat. Struct. Biol. *7*, 800–807.

Wahl, J.K.I., Nieset, J.E., Sacco-Bubulya, P.A., Sadler, T.M., Johnson, K.R., and Wheelock, M.J. (2000). The amino- and carboxyl-terminal tails of β-catenin reduce its affinity for desmoglein 2. J. Cell Sci. *113*, 1737–1745.

Witcher, L.L., Collins, R., Puttagunta, S., Mechanic, S.E., Munson, M., Gumbiner, B., and Cowin, P. (1996). Desmosomal cadherin binding domains of plakoglobin. J. Biol. Chem. *271*, 10904–10909.

Yap, A.S., Brieher, W.M., and Gumbiner, B.M. (1997a). Molecular and functional analysis of cadherin-based adherens junctions. Annu. Rev. Cell Dev. Biol. *13*, 119–146.

Yap, A.S., Brieher, W.M., Pruschy, M., and Gumbiner, B.M. (1997b). Lateral clustering of the adhesive ectodomain: a fundamental determinant of cadherin function. Curr. Biol. *7*, 308–315.

Yap, A.S., Niessen, C.M., and Gumbiner, B.M. (1998). The juxtamembrane region of the cadherin cytoplasmic tail supports lateral clustering, adhesive strengthening, and interaction with $p120^{ctn}$. J. Cell Biol. *141*, 779–789.

Accession Numbers

Coordinates and structure factors for both E_{cyto}/β-catenin and phos-E_{cyto}/β-catenin have been deposited in the Protein Data Bank, with accession codes 1I7X and 1I7W, respectively.